Published in final edited form as:
Technol Innov. 2014 ; 16(1): 55–62. doi:10.3727/194982414X13971392823398.

QUANTITATIVE MORPHOLOGICAL AND MOLECULAR PATHOLOGY OF THE HUMAN THYMUS CORRELATE WITH INFANT CAUSE OF DEATH

Mark C. Lloyd[*], **Nancy Burke**[*], **Fatemeh Kalantarpour**[†], **Melissa I. Niesen**[‡], **Aaron Hall**[§], **Keith Pennypacker**[§], **Bruce Citron**[‡,¶], **Chaim G. Pick**[#], **Vernard Adams**[**,††], **Mahasweta Das**[‡‡], **Shyam Mohapatra**[‡‡], **Hernani Cualing**[††,§§], and **George Blanck**[†,‡]

[*]Analytic Microscopy Core, H. Lee Moffitt Cancer Center and Research Institute, Tampa, FL, USA

[†]Department of Oncological Sciences, H. Lee Moffitt Cancer Center and Research Institute, Tampa, FL, USA

[‡]Department of Molecular Medicine, University of South Florida, Tampa, FL, USA

[§]Department of Molecular Pharmacology and Physiology, University of South Florida, Tampa, FL, USA

[¶]Laboratory of Molecular Biology, Bay Pines VA Healthcare System, Bay Pines, FL, USA

[#]Department of Anatomy and Anthropology, Tel Aviv University, Tel Aviv, Israel

[**]Medical Examiner Department, Hillsborough County Government, Tampa, FL, USA

[††]Department of Pathology and Cell Biology, University of South Florida, Tampa, FL, USA

[‡‡]Department of Internal Medicine, University of South Florida, Tampa, FL, USA

[§§]IHCFLOW, Inc., Lutz, FL, USA

Abstract

The objective of this study was to investigate and quantify the morphological and molecular changes in the thymus for common causes of human infant death. Thymic architecture and molecular changes apparent in human infant head trauma victims were assessed by microscopy and quantified by image analysis of digital whole slide images. Thymuses from victims of SIDS and suffocated infants displaying normal thymus architecture were used for comparison. Molecular expression of proliferation and serotonin receptor and transporter protein markers was evaluated. Duplicate morphological and molecular studies of rodent thymuses were completed with both mouse and rat models. Quantification of novel parameters of digital images of thymuses from human infants suffering mortal head trauma revealed a disruption of the corticomedullary organization of the thymus, particularly involving dissolution of the corticomedullary border. A similar result was obtained for related mouse and rat models. The human thymuses from head

Address correspondence to George Blanck, 12901 Bruce B. Downs Blvd., MDC7, Tampa, FL 33612, USA. Tel: +1-813-974-9585; gblanck@health.usf.edu.

The authors declare no conflict of interest.

trauma cases also displayed a higher percentage of Ki-67-positive thymocytes. Finally, we determined that thymus expression of the human serotonin receptor, and the serotonin transporter, occur almost exclusively in the thymic medulla. Head trauma leads to a disruption of the thymic, corticomedullary border, and molecular expression patterns in a robust and quantifiable manner.

Keywords

Head trauma; Thymus gland; Infant; T-cells; Serotonin; Serotonin receptor; Quantitative pathology

BACKGROUND

The goal of this study was to determine differences in thymus from infants whose cause of death was reported as sudden infant death syndrome (SIDS) compared to those dying from events of suffocation or head trauma (10). The implications of a quantifiable metric for determining infant death may provide medical examiners with important information that can be used to support an infant's autopsy report. Furthermore, these studies began to unravel interesting questions of biological importance regarding changes in the thymus following mortal injury events.

These quantifiable measures were made possible via the rapidly expanding field of quantitative image analysis. This discipline enables subject matter experts to measure and quantify commonly observed phenomena, such as thymic structure and molecular expression (8,14). Historically, anatomic pathology has been analyzed qualitatively for diagnosis. However, in the last decade, great strides have been made toward increased quantification of anatomic pathology leading a paradigm shift toward precision pathology using digital images and powerful computational algorithms. In this case, precision pathology extends into the field of forensic pathology. For decades, forensic pathologists have also used qualitative descriptions of their observations (13). A prime example can be made of the thymic architecture including descriptors such as "starry sky," given the increase in interstitial space (12). Until recently, phenotypic quantification of features of single cells has been largely ignored by clinicians and investigators due to technological limitations. However, with the advent of high-content automated slide scanning coupled with cognitive and scriptable algorithms, researchers are well poised to identify and quantify single cell features to provide insight into disease as well as cause of death.

While a great deal of work has recently been directed toward the impact of brain function and head trauma on the immune system, very little is known regarding the effect of head trauma on the thymus, the site of maturation and negative selection of T-cells, or the source of circulating T-cells (1,4,9). Here we examined the thymuses of human infants deceased from brain trauma and observed that these thymuses had disrupted architecture and a significant dissolution of the corticomedullary border (compared to infants deceased from suffocation or SIDS) using digital pathology for acquisition and analysis of morphological features (15). Furthermore, while proliferation is studied in other pathologies, information regarding thymic activity and head trauma is underappreciated (5,16). We evaluated head

trauma, which was found to correlate with an increase in Ki-67 staining of thymocytes, indicating the induction of a proliferative response.

MATERIALS AND METHODS

Histology and Image Acquisition

Under the auspices of the University of South Florida Institutional Review Board, human infant thymuses from autopsy cases were reviewed. In each of the six cases, the autopsies were performed a maximum of 36 h postmortem. Paraffin-embedded, formalin-fixed tissues were prepared for microscopy as described, sections were stained with hematoxylin and eosin (H&E), and immunohistochemistry was performed with rabbit polyclonal anti-serotonin receptor-1A and anti-serotonin reuptake transporter (SERT) (2). Slides were scanned using the Aperio™ (Vista, CA) ScanScope XT with a 20 × /0.8 NA objective lens at a rate of 2 min per slide via Basler trilinear array.

Morphological Image Analysis

Image analysis was performed using a Positive Pixel Count v9.1 algorithm with the following customized thresholds [hue value = 0.2; hue width = 0.6; color saturation threshold = 0.05; Iwp (high) = 210; Iwp (low) = Ip (high) = 160; Ip (low) = Isp (high) = 80; Isp (low) = 0]. The algorithm was applied to the entire scanned slide image to detect regions of increased interstitial space by detecting pixels that satisfy the color and intensity specification defined above. Data were combined by condition, and the ratio of interstitial space over total area was defined by pixels and plotted as bar graphs in Figures 1 and 2. Line profile traces were objectively applied across cortical and medullar border regions at 0°, 45°, and 90° to graphically represent border integrity retention across each sample type (Fig. 3A-C) using gray scale image sets.

Experimental Injury

The mouse head trauma model uses a dropping weight that delivers a noninvasive, closed-skull injury to the brains of the 19 mice. At the time of injury, mice were lightly anesthetized with isoflurane and placed on a sponge underneath a metal tube (13 mm diameter × 80 cm long) so that the impact to the skull would be immediately anterior to the right ear. The metal weight was dropped down the tube and struck the temporal region of the skull.

After the trauma was delivered to the mouse brains by the fluid percussion injury device, the mice were allowed to recover in their home cage and allowed to survive for 24 or 48 h. After the survival period, they were deeply anesthetized and transcardially perfused with 0.9% saline followed by 4% paraformaldehyde. Sham animals were also perfused in the same way and at the same time points. Brains were removed after perfusion fixation. Thymuses were removed before perfusion, washed in 0.9% saline, and post-fixed in 4% paraformaldehyde for histological preparation. Some preliminary experiments were done with an alternative mouse head trauma model (17).

Permanent rat middle cerebral artery occlusion (MCAO) procedures were done as described by Leonardo et al. (6). Briefly, eight male rats of 200 to 250 g (between 6.5 and 7.5 weeks

of age) were anesthetized in an induction chamber with 3% to 4% isoflurane in oxygen. Anesthesia was maintained with 2.5% to 3% isoflurane in oxygen delivered at 1 L per minute. The carotid bifurcation was exposed by incising the skin and fascia ventral to the right sternocleidomastoid muscle. The vagus nerve was dissected free of the right common carotid artery before the common carotid artery was clamped. Two 5-0 ligatures, one distal and one proximal, were used to cinch the external carotid artery closed, following which the artery was transected between the ligatures. Branches of the external carotid artery were cauterized, as needed, to control bleeding. The proximal ligated stump of the external carotid artery was then used as a portal to pass an occluder (fishing line) into the lumen of the internal carotid artery as follows. The proximal stump of the external carotid artery was perforated with a 40-mm length of 6-pound test monofilament, which was then introduced into the lumen of the carotid bifurcation and thence into the internal carotid artery. This occluder was fed rostrally through the middle cerebral artery (MCA) until resistance was met (typically at about 25 mm), signaling complete occlusion of the MCA. At this time, the occluder was permanently secured, the clamp on the common carotid was removed, and Gelfoam® was placed over the carotid fascia. A laser Doppler monitor was used to determine reductions in blood flow. Animals that did not show at least 60% reduction in blood flow following introduction of the occluder were excluded from the study. The mouse and rat model experiments were approved by the University of South Florida Institutional Animal Care and Use Committee (IACUC).

Immunohistochemical Image Analysis

To accurately and efficiently assess Ki-67 expression in immunostained thymus tissue, we used the VirtualFlow™ technique (IHCFLOW, Inc., Tampa, FL). This software generates a two-parameter dot-plot display, similar to those generated in flow cytometry. The microscopic images were captured using a 20×, 0.4 NA objective (Leica, Wetzlar, Germany) and a color brightfield CCD high-resolution camera (Diagnostic Instruments). Each image is 512 × 474 pixels, with 1.5 pixels per micron. No manual or interactive labeling or shading or color correction was performed. The light intensity rheostat was set to 7.0 of 12.0. The light source was a 30-W 12-V incandescent bulb with a condenser blue filter, 80a Tiffen, with the condenser aperture set a 0.5 ph. This method automatically converts digital images of immunostained tissue to percentage positive, using a multithresholding, iterative bit slice identification of stained nuclei and unstained nuclei. The single cell count results correlate with both manual Ki-67 scoring and standardized tissue flow cytometry results (3). Briefly, thymic sections, previously immunostained as described, using Ki-67 AP-DAB (Mib-1, Ventana) by automated Ventana XT (Tucson, AZ, USA) are put on the stage (2). The nuclei (brown stained) and hematoxylin (blue counterstained) image plane is manually focused, captured, and saved as a JPEG file. Segmentation and display of histogram and statistical results table take 3 to 4 s. An average of 40 frames (with 329 to 811 cells per frame) was captured per slide on all thymic cortex and medulla regions. Results were tabulated and analyzed per region and per subject thymus using ANOVA (GraphPad software).

RESULTS

We obtained a series of thymus samples from human infants deceased from head trauma, SIDS, or suffocation. Upon analysis of the sample set, two observations were made. First, the expression of both the serotonin receptor-1A and SERT were highly concentrated in the medulla of all samples. Second, thymuses from head trauma were highly disorganized, particularly having extensive interstitial space among the thymocytes and a disrupted corticomedullary border (Fig. 4A-C), the region of entry of pre-T-cells into the thymus (11). This appearance has been referred to as a “starry sky” or marbled appearance for thymuses representing other pathological situations. To statistically assess the distinctions between the head trauma thymuses and the suffocation/SIDS thymuses, the interstitial space was quantified as indicated in the Materials and Methods section, revealing a statistically significant difference (Fig. 1). Furthermore, disruption of the border could be represented by a line trace, providing an alternative quantitative comparison of the border integrity for different samples (Fig. 3A-C).

To support the conclusion that thymus disruption correlated with head trauma and to establish an animal model for future studies, we employed a mouse head trauma model as described in the Materials and Methods section. Analysis of H&E-stained thymus sections showed that thymuses from mice receiving head trauma had a significantly increased level of interstitial space compared to sham-treated mice (Fig. 2). A qualitative assessment of a rat stroke model (Materials and Methods) gave a similar result (Fig. 5).

To begin to assess the molecular and cellular changes underlying the disorganization of the thymus associated with head trauma, we stained thymuses with anti-Ki-67. We found a 29.5% increase in Ki-67-positive thymocytes in the thymuses from head trauma victims (Fig. 6A, B and Fig. 7).

CONCLUSIONS

These results indicate that serotonin receptor-1A expression and SERT expression on thymocytes is concentrated in the medulla, where mature T-cells reside. The role of serotonin in T-cell function remains to be elucidated, but in general, reports indicate that serotonin exposure leads to or facilitates T-cell activation (7).

The results described above also indicate that head trauma leads to a disruption of thymus architecture, which can be quantified as increased interstitial space between the thymocytes and a disruption of the corticomedullary border. The authors do not have direct empirical evidence to explain why there is an increase in interstitial space between thymocytes; however, we do offer one hypothesis. Head trauma may result in massive exit of the cells from the thymus. It is known that the corticomedullary border is the site of exit, and this would explain its disruption. Future work will test this hypothesis.

Head trauma was also associated with an increase in Ki-67-positive thymocytes, representing a significant 30% increase in thymocytes undergoing DNA replication. Future studies will be oriented toward understanding the mechanism of the effect of head trauma on the thymus and the implications for the effect of head trauma on the immune system. For

example, does nonfatal head trauma reduce apoptosis of self-reactive thymocytes or affect the number of self-reactive thymocytes entering the periphery?

Furthermore, it becomes possible to describe how these quantified metrics of change in the thymus may be able to infer important information with health implications of this study. Metrics of thymic integrity may be used to confirm the cause of death in infant autopsies, measure chronic head trauma impacts, or a number of other biomedical applications.

Acknowledgments

We thank the Analytic Microscopy Core at the Moffitt Cancer Center and John S. Dennis for technical assistance. We also thank Dr. Leszek Chrostowski for helpful discussions. This work was supported by a grant from the Florida Biomedical Research Program (GB), by the Department of Veterans Affairs and the Bay Pines Foundation (BC), by the VA Career Scientist Award, and by the Mabel and Ellsworth Simmons Professorship at the USF College of Medicine (SM).

REFERENCES

1. Chilosi M, Iannucci A, Menestrina F, Lestani M, Scarpa A, Bonetti F, Janossy G. Immunohistochemical evidence of active thymocyte proliferation in thymoma: Its possible role in the pathogenesis of autoimmune diseases. Am. J. Pathol. 1987; 128(3):464–470. [PubMed: 2443011]
2. Coppola D, Parikh V, Boulware D, Blanck G. Substantially reduced expression of PIAS1 is associated with colon cancer development. J. Cancer Res. Clin. Oncol. 2009; 135:1287–1291. [PubMed: 19288270]
3. Cualing HD, Zhong E, Moscinski L. Virtual flow cytometry of immunostained lymphocytes on microscopic tissue slides: iHCFlow tissue cytometry. Cytometry B Clin. Cytom. 2007; 72:63–76. [PubMed: 17133379]
4. Halvorson MJ, Coligan JE. Enhancement of VLA integrin receptor function on thymocytes by cAMP is dependent on the maturation stage of the thymocytes. J. Immunol. 1995; 155(10):4567–4574. [PubMed: 7594454]
5. Kvetnoy IM, Polyakova VO, Trofimov AV, Yuzhakov VV, Yarilin AA, Kurilets ES, Mikhina LN, Sharova NI, Nikonova MF. Hormonal function and proliferative activity of thymic cells in humans: Immunocytochemical correlations. Neuro Endocrinol. Lett. 2003; 24(3-4):263–268. [PubMed: 14523368]
6. Leonardo CC, Hall AA, Collier LA, Green SM, Willing AE, Pennypacker KR. Administration of a sigma receptor agonist delays MCAO-induced neurodegeneration and white matter injury. Transl. Stroke Res. 2010; 1(2):135–145. [PubMed: 20563232]
7. Levite M. Neurotransmitters activate T-cells and elicit crucial functions via neurotransmitter receptors. Curr. Opin. Pharmacol. 2008; 8:460–471. [PubMed: 18579442]
8. Lloyd MC, Allam-Nandyala P, Purohit CN, Burke N, Coppola D, Bui MM. Using image analysis as a tool for assessment of prognostic and predictive biomarkers for breast cancer: How reliable is it? J. Pathol. Inform. 2010:1. [PubMed: 20805964]
9. Morganti-Kossmann MC, Satgunaseelan L, Bye N, Kossmann T. Modulation of immune response by head injury. Injury. 2007; 38:1392–1400. [PubMed: 18048036]
10. Paterson DS, Trachtenberg FL, Thompson EG, Belliveau RA, Beggs AH, Darnall R, Chadwick AE, Krous HF, Kinney HC. Multiple serotonergic brainstem abnormalities in sudden infant death syndrome. JAMA. 2006; 296:2124–2132. [PubMed: 17077377]
11. Penit C, Vasseur F. Sequential events in thymocyte differentiation and thymus regeneration revealed by a combination of bromodeoxyuridine DNA labeling and antimitotic drug treatment. J. Immunol. 1988; 140:3315–3323. [PubMed: 3258880]
12. Tsibel BN, Bochkareva AK. Functional morphology of adenohypophysis, thymus, and adrenal cortex in sudden infant death syndrome. Arkhiv. Patologii. 1998; 60(2):23. [PubMed: 9612505]

13. van Baarlen J, Schuurman HJ, Huber J. Acute thymus involution in infancy and childhood: A reliable marker for duration of acute illness. Hum. Pathol. 1988; 19(10):1155–1160. [PubMed: 3169723]

14. Werlen G, Hausmann B, Naeher D, Palmer E. Signaling life and death in the thymus: Timing is everything. Science. 2003; 299(5614):1859–1863. [PubMed: 12649474]

15. Willinger M, James LS, Catz C. Defining the sudden infant death syndrome (Sids): Deliberations of an expert panel convened by the National Institute of Child Health and Human Development. Fetal Pediatr. Pathol. 1991; 11(5):677–684.

16. Yang WI, Efird JT, Quintanilla-Martinez L, Choi N, Harris NL. Cell kinetic study of thymic epithelial tumors using PCNA (PC10) and Ki-67 (MIB-1) antibodies. Hum. Pathol. 1996; 27(1): 70–76. [PubMed: 8543314]

17. Zohar O, Schreiber S, Getslev V, Schwartz JP, Mullins PG, Pick CG. Closed-head minimal traumatic brain injury produces long-term cognitive deficits in mice. Neuroscience. 2003; 118:949–955. [PubMed: 12732240]

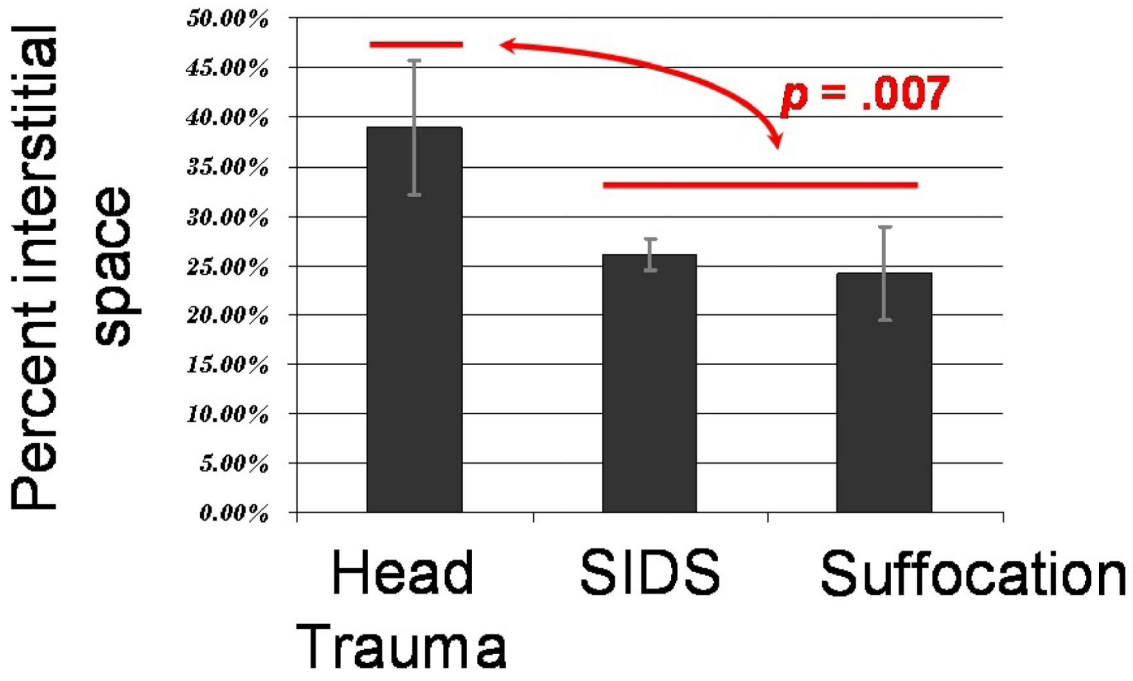

Figure 1.
Quantification of the percent interstitial space between thymocytes in human head trauma, suffocation, and SIDS thymuses.

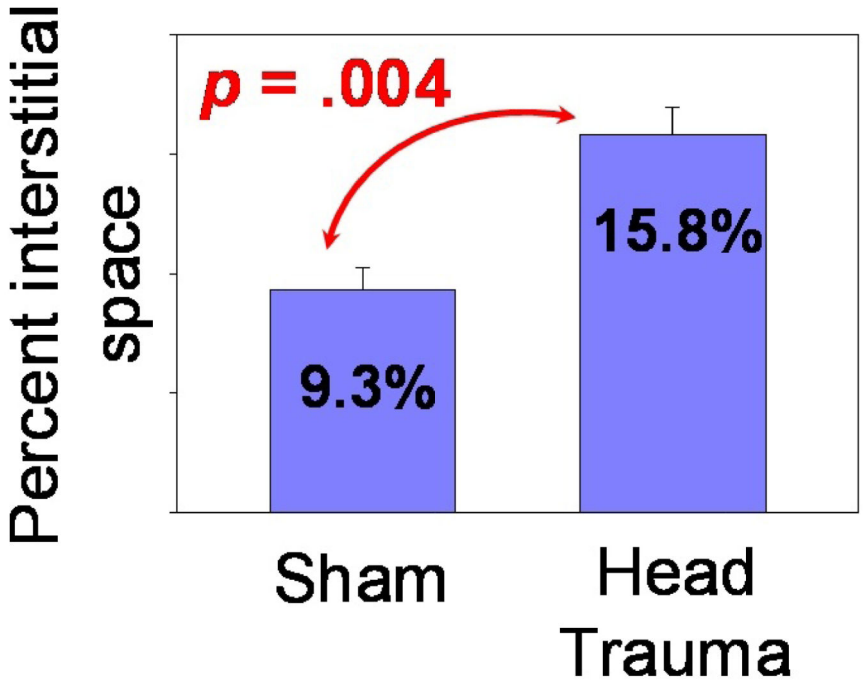

Figure 2.
Quantification of the percent interstitial space in mouse thymuses with head trauma and sham-treated animals.

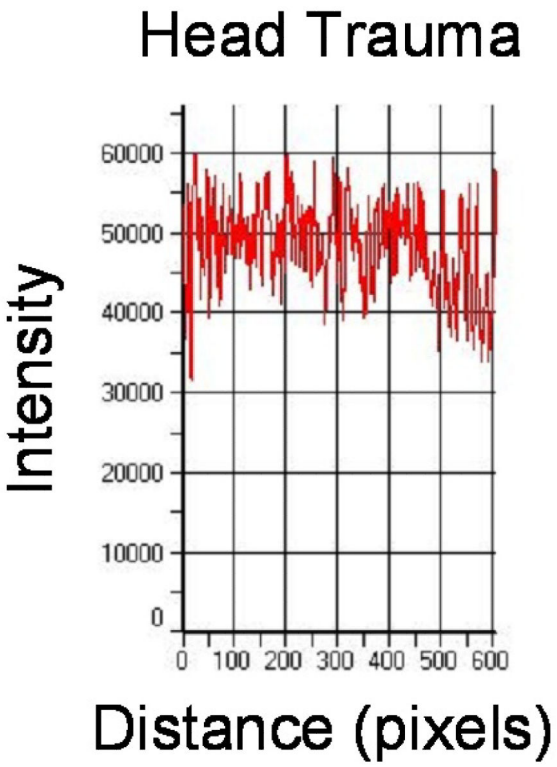

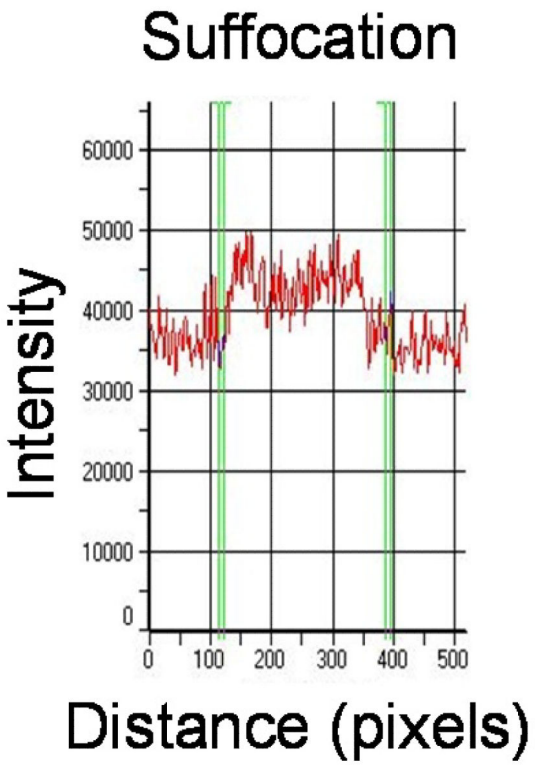

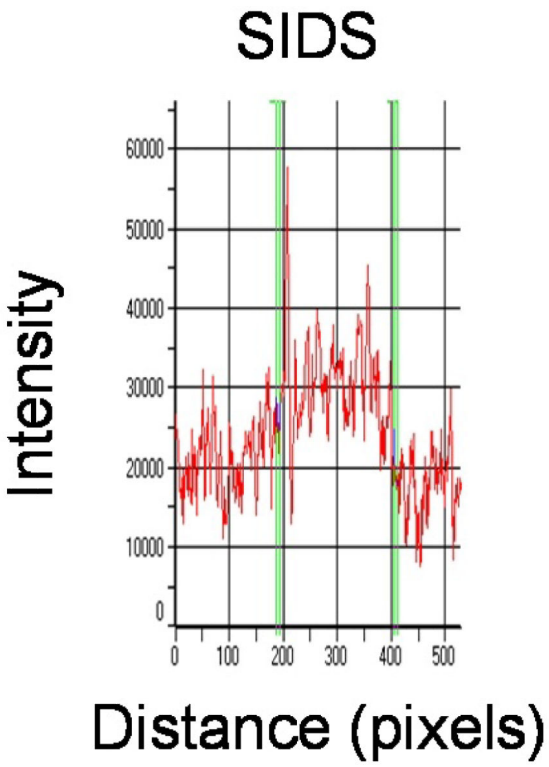

Figure 3.

These figures show intensity as a function of distance (pixel) for (A) head trauma, (B) suffocation, and (C) SIDS. This plot indicates the extent of corticomedullary border integrity in individual lobules of human thymuses.

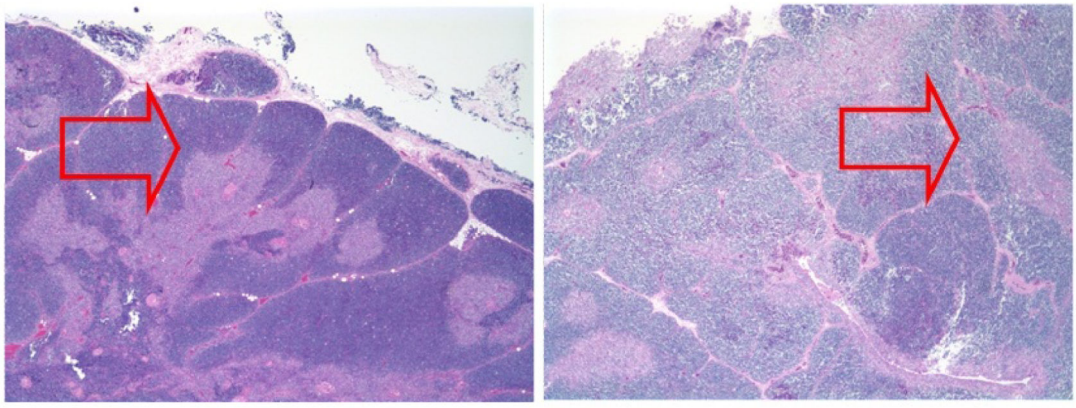

Suffocation Head Trauma

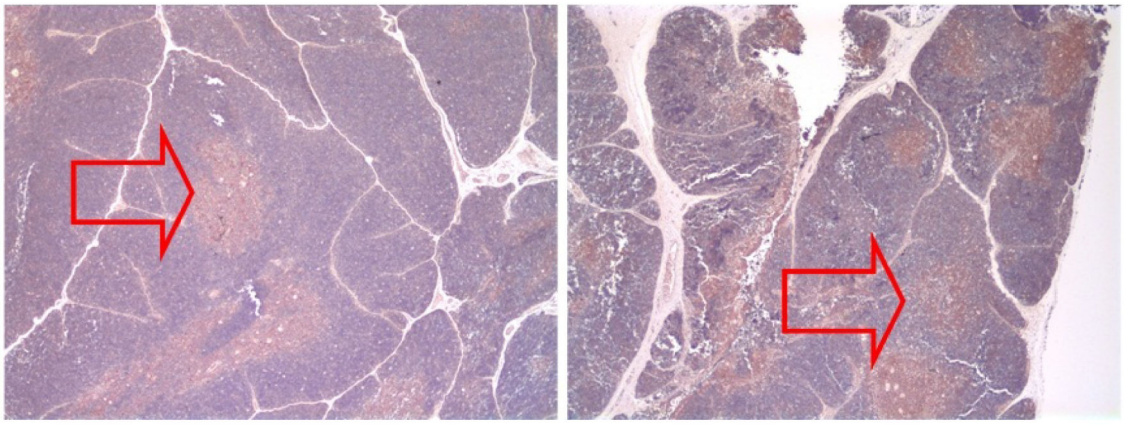

Suffocation Head Trauma

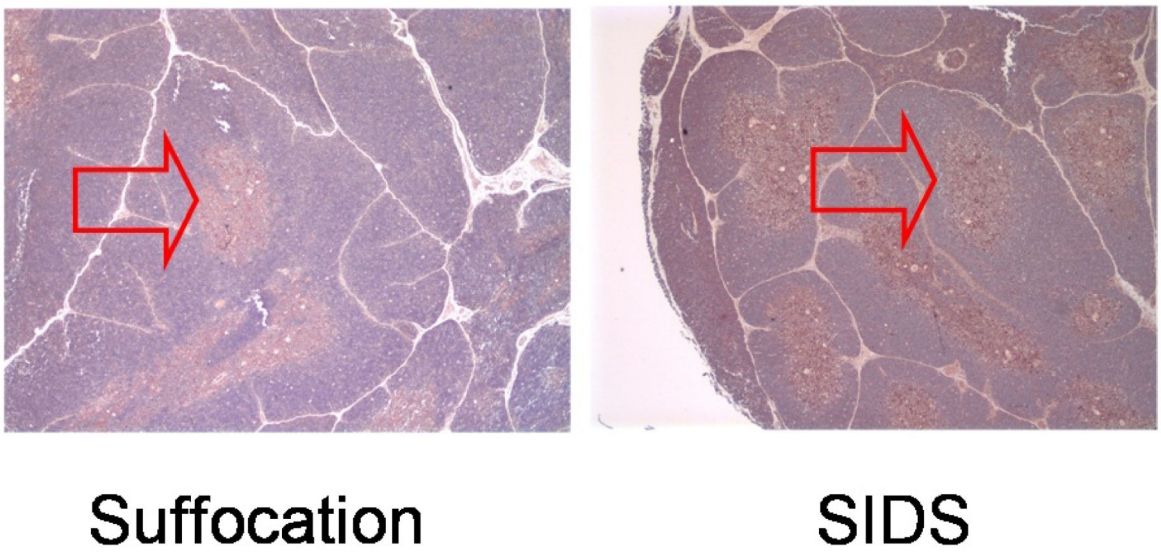

Figure 4.

(A) H&E stain of human thymuses from infants suffering fatal suffocation (left) or head trauma (right). Arrows indicate intact corticomedullary architecture and disrupted corticomedullary architecture in suffocation and head trauma, respectively. (B) SERT staining of thymuses from infants suffering fatal suffocation (left) or head trauma (right). Arrows indicate largely medullary-specific staining or diffuse staining, in suffocation and head trauma, respectively. (C) SERT staining of thymuses from infants suffering fatal suffocation (left) or SIDS (right). Arrows indicate largely medullary-specific staining in both images.

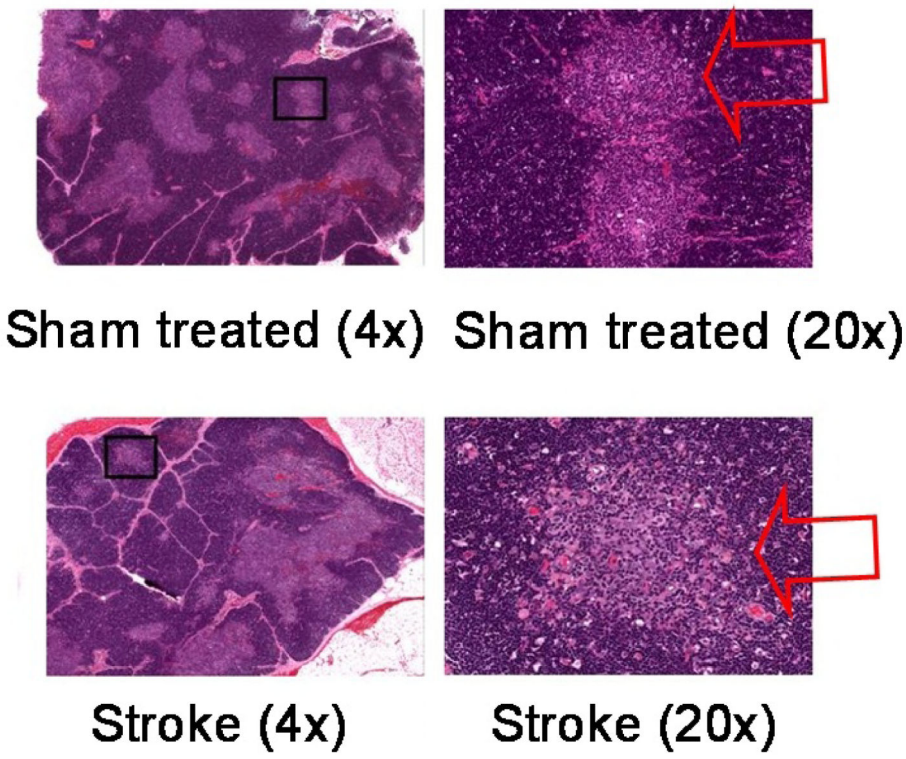

Figure 5.
Representative micrographs of the thymus medulla and cortex from a sham-treated and rat stroke model. Arrows indicate sharp or diffuse corticomedullary border in sham and stroke rats, respectively.

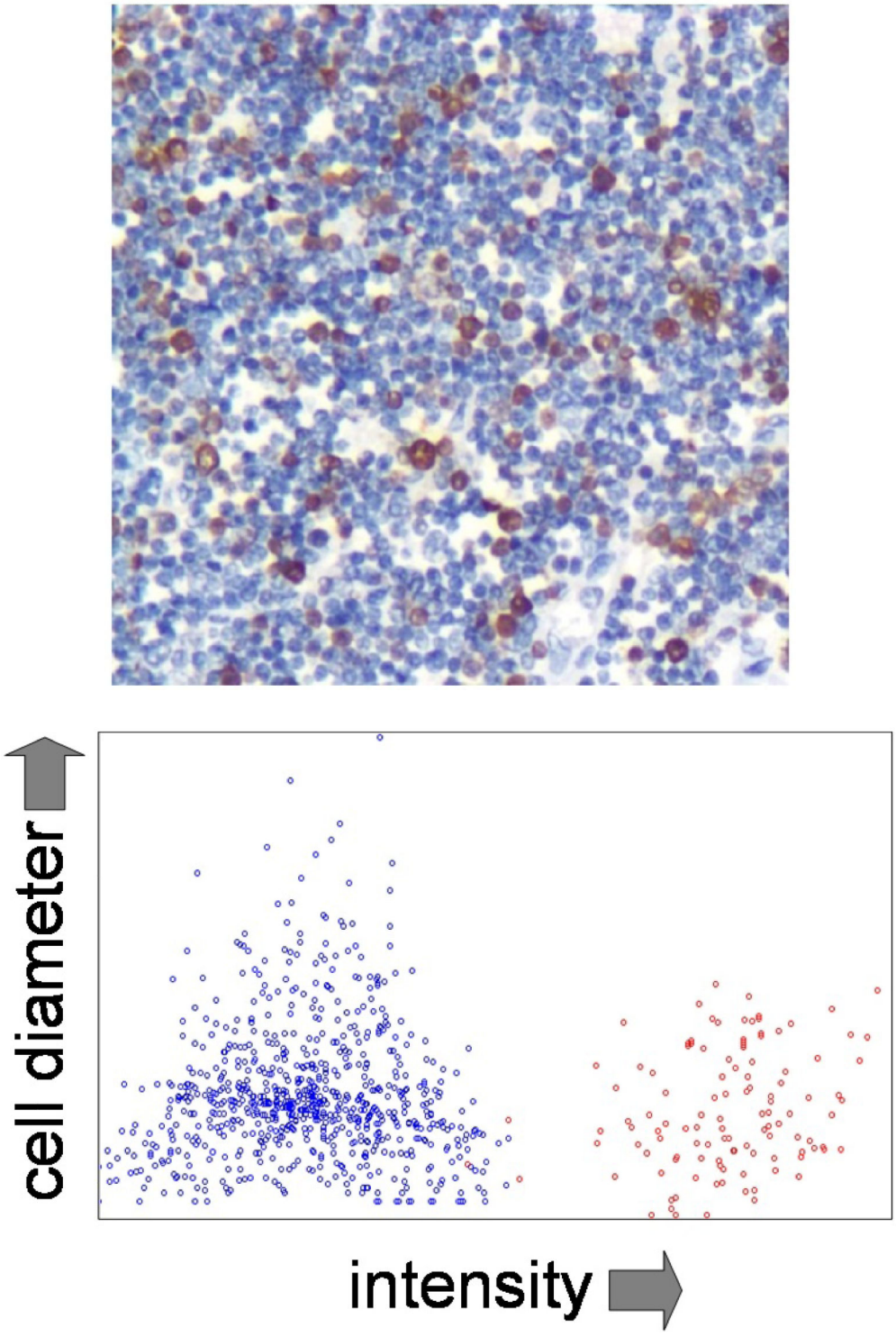

Figure 6.
(A) Example Ki-67 staining of a human thymus. (B) Virtual flow results from (A).

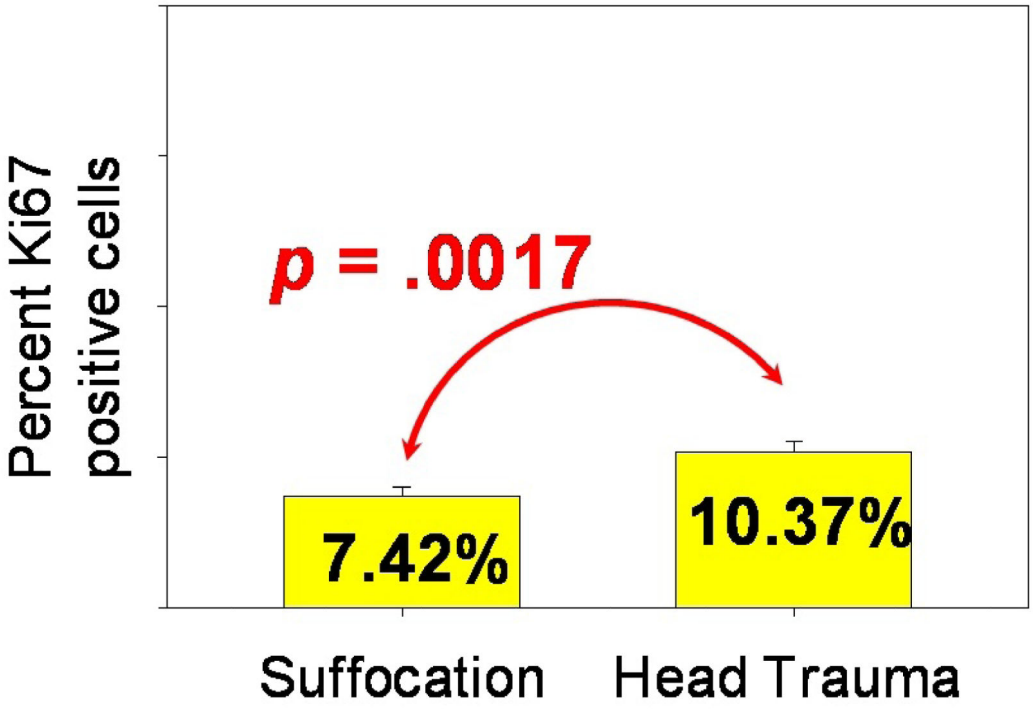

Figure 7.
Quantification of percent Ki-67-positive cells in staining in thymuses from human head trauma and suffocation.